materials

MDPI

Article

Mix Proportion Design of Self-Compacting SFRC with Manufactured Sand Based on the Steel Fiber Aggregate Skeleton Packing Test

Xinxin Ding [1,2,*], Minglei Zhao [3], Jie Li [3,*], Pengran Shang [1,2] and Changyong Li [1,2]

[1] International Joint Research Lab for Eco-building Materials and Engineering of Henan, North China University of Water Resources and Electric Power, Zhengzhou 450045, China; pr.shang@st.ncwu.edu.cn (P.S.); lichang@ncwu.edu.cn (C.L.)

[2] School of Civil Engineering and Communication, North China University of Water Resources and Electric Power, Zhengzhou 450045, China

[3] School of Engineering, RMIT University, Melbourne, VIC 3001, Australia; s3339909@student.rmit.edu.au

* Correspondence: dingxinxin@ncwu.edu.cn (X.D.); Jie.li@rmit.edu.au (J.L.); Tel.: +86-371-6912-7377 (X.D.)

Received: 5 May 2020; Accepted: 22 June 2020; Published: 24 June 2020



Abstract: A scientific and concise mix design method is an impending problem in the engineering application of self-compacting steel-fiber-reinforced concrete (SFRC). This paper focuses on the mix proportion of self-compacting SFRC, which is influenced by the steel fibers, along with its effects on the packing properties of the steel fiber aggregate skeleton. In total, 252 groups of packing tests were carried out for several main factors, including with various maximum particle sizes for the coarse aggregates, manufactured sand ratios ranging from 50% to 62%, and with different types of hooked-end steel fibers and crimped steel fibers, with volume fractions ranging from 0% to 2.0%. The results indicated that the void content and rational sand ratio of the steel fiber aggregate skeleton increased linearly with the fiber factor. These results provided a basis for the calculation of the binder content and rational sand ratio of the self-compacting SFRC. Combined with the absolute volume design method and the calculation formula for the water-to-binder ratio, a systematical procedure was proposed for the mix proportion design of the self-compacting SFRC. Based on the design method, eight groups of mixtures were cast and tested to verify the adaptability and practicability of the workability, air content, density, cubic compressive strength, and splitting tensile strength of the self-compacting SFRC. Meanwhile, the outcomes of this study confirmed the applicability of using manufactured sand as a complete replacement for natural sand for the self-compacting SFRC.

Keywords: self-compacting SFRC; mix design method; steel fiber aggregate skeleton; void content; manufactured sand ratio; verification test

1. Introduction

Fresh self-compacting steel-fiber-reinforced concrete (SFRC) can be considered as a compound consisting of a continuous liquid phase of binder paste and a dispersed solid phase of coarse aggregate, fine aggregate, and steel fibers. As these two phases function differently in terms of the flowability of fresh self-compacting SFRC and the properties of hardened self-compacting SFRC, previous research studies have mainly focused on the performance and volume percentage of the binder paste and solid phase [1]. Differing from granular aggregates, steel fibers have a distinctive elongated shape. This results in a more complex mix design for self-compacting SFRC to ensure stable workability and satisfactory strengths than that of self-compacting concrete (SCC) [2–4].

Until now, the mix proportion design for self-compacting SFRC has been done by modifying the mix proportions of SCC. Different measures have been used, as follows:

(1) A simplified mix design method, in which steel fibers are added directly into the SCC mixture without optimizing the bulk density. The required workability and mechanical performance of self-compacting SFRC can be satisfied by properly adjusting the dosage or type of superplasticizer [5], the proportion of cement and chemical admixtures [6–9], the sand ratio, and the binder content [10], or even without any change of the components in the reference SCC [11,12]. This method is simple but poorly reproducible, and is heavily dependent on the experience of technicians.

(2) A mixture design algorithm method is used to successively fill voids among the coarse aggregate and sand by using sand and fly ash to densely pack the aggregates [13]. The volume of steel fibers is regarded as a part of the solid volume filling the voids in the aggregate skeleton. The cement paste is considered to be the lubricating paste, which has a certain thickness and is wrapped around the aggregates. By using the absolute volume method, the dosages of each composite can be computed. Finally, proper adjustments are carried out according to the requirements of the properties of fresh and hardened self-compacting SFRCs. This method requires iterative packing tests to obtain the maximum dry loose density of the granular aggregates and does not consider the effect of the distinctive elongated shape of the steel fibers on the packing patterns of the granular skeleton.

(3) The compressible packing model for SCC is modified for the optimization of the fiber aggregate skeleton in order to calculate the actual bulk density [1,14,15]. In view of the aspect ratio and diameter, steel fibers are counted in the granular skeleton as the equivalent packing diameter and the boundary effect on the bulk density of steel fibers is computed. In this method, three steps have to be followed to determine the bulk density of one group or polydisperse groups of grains or fibers.

(4) The rheology paste model for SCC is modified for the self-compacting SFRC [16,17]. Through the equivalent diameter concept for steel fibers with the same specific surface, steel fibers are included in the particle size distribution of the granular skeleton. Based on the optimization of the SCC paste model, the rheological and mechanical behaviors are evaluated using the design of the experiment method to identify the composition factors, including the optimized sand ratio and paste volume for self-compacting SFRC, along with a constant fiber factor [18].

(5) Combined with the optimized fiber aggregate skeleton and based on the packing tests, the minimum amount of binder paste is determined according to the self-compacting performance requirements [19–21]. In this method, the influence of the steel fiber on the fiber aggregate skeleton is evaluated. However, more experiments need to be conducted to determine the mix proportion of self-compacting SFRC.

(6) The self-compacting SFRC is made up of the SCC matrix and steel fiber cement paste [22]. Additionally, the SCC matrix is prepared based on the rheological parameters of the basic mortar, which is derived from the SCC matrix, and the steel fiber cement paste is prepared based on the average paste film thickness. This method is suitable for self-compacting concrete containing microsteel fibers. The fiber factor no more than 0.7.

(7) Some researchers have proposed certain parameters using the Taguchi method or even by changing the nature of raw materials to simplify and optimize the mix proportions of self-compacting SFRCs. The dry mortar ratio was proposed to control the proportion and composition of the concrete matrix to involve steel fibers, resulting in a mixture with self-compacting properties [23]. The Taguchi orthogonal array method has been reported for the optimization of the mix proportion design of self-compacting SFRCs [24]. Self-compacting SFRCs mixed with magnetized water have also been reported to have improved fresh and hardened state properties [25].

Due to lack of a unified method, only the design principles have been proposed in the specifications and guidelines for the mix design of self-compacting SFRCs. The European Guidelines [26] emphasize that the selection of the type, length, and volume fraction of steel fibers depends on the maximum size of the aggregate and the structural requirements. Experiments are needed to determine the optimum results. Combined with the specifications for fiber-reinforced concrete in BS EN 14889-1 [27] and the specifications for SCCs in the European Guidelines [26], British standard BS EN 206-9 [28] proposes the mix design procedure for self-compacting SFRC. In China, the mix design for self-compacting SFRC is

normally based on repeated experiments, referencing the workability requirements of SCC in JGJ/T 283 [29], the test methods in CECS 13 [30], and the mechanical properties requirements for SFRCs in JG/T 472 [31] and JGJ/T 221 [32]. Therefore, the lack of a scientific and concise mix design method is still an important problem in the application of self-compacting SFRC.

Meanwhile, with the exhaustive use of river sand harming the natural environment, manufactured sand has become an effective replacement for river sand in concrete. The application of manufactured sand in SCC and self-compacting SFRC is inevitable. As the morphology of manufactured sand is different from river sand, this obviously has an influence on the workability and mechanical properties of concrete [33,34]. This increases the difficulty of the mix proportion design for self-compacting SFRC with manufactured sand.

Based on the above analyses, this study focuses on the mix proportion design method for self-compacting SFRCs with manufactured sand. In total, 252 groups of packing tests were carried out to investigate the effects of steel fibers on the packing properties of the steel fiber aggregate skeleton with various manufactured sand ratios, ranging from 50% to 62%. Hooked-end steel fibers with different lengths and crimped steel fibers were used, with volume fractions ranging from 0% to 2.0%. Relationships between the void content and the rational sand ratio of the steel fiber aggregate skeleton considering the fiber factor were obtained, which provided the basis for the calculation formulas. Combined with the absolute volume design method and the calculation formula for the water-to-binder ratio [35,36], a systematical procedure was proposed for the mix proportion design of self-compacting SFRC. The adaptability and practicability of the design method in terms of the workability, air content, density, cubic compressive strength, and splitting tensile strength of self-compacting SFRC were confirmed by the verification tests.

2. Packing Tests of the Steel Fiber Aggregate Skeleton

2.1. Raw Materials

As displayed in Figure 1, three types of hooked-end steel fibers with different aspect ratios (HFa, HFb, and HFc) and one type of crimped steel fiber (CF) were used in the packing test. Their physical and mechanical properties are presented in Table 1.

The coarse aggregate was the crushed limestone, containing maximum particle sizes (MPS) of 10, 16, and 20 mm. The basic mechanical and physical properties were tested according to Chinese standard JGJ 52 [37] and are presented in Table 2. The particle size distributions are presented in Figure 2.

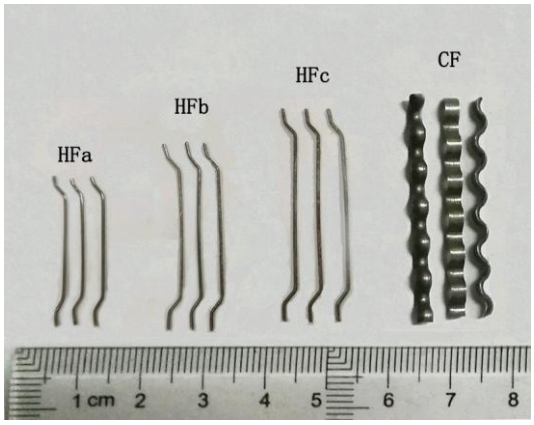


Figure 1. Steel fibers.

Table 1. Physical and mechanical properties of steel fibers. HF, hooked-end steel fiber; CF, crimped steel fiber.

No.		HFa	HFb	HFc	CF
Type		Hooked-end			Crimped
Cross-section	Shape	circle			rectangle
	Circumference (mm)	1.57			5.33
Length l_f (mm)		25	30	35	38.8
Equivalent Diameter d_f (mm)		0.50	0.50	0.50	1.17
Aspect Ratio l_f/d_f		50	60	70	33
Number of Steel Fibers Per Kilogram N_{sf} (per kg)		25,861	21,637	18,546	3347
Tensile Strength (MPa)		1150	1150	1150	800

Table 2. Physical and mechanical properties of crushed limestone.

Maximum Particle Size (MPS) (mm)	Apparent Density (kg/m^3)	Loose Bulk Density (kg/m^3)	Dense Bulk Density (kg/m^3)	Crushed Index (%)	Mud Content (%)	Content of Needle Pieces (%)
10	2720	1490	1530	-	0.6	4.9
16	2736	1529	1591	12.2	0.5	5.3
20	2713	1543	1647	9.0	0.4	6.0

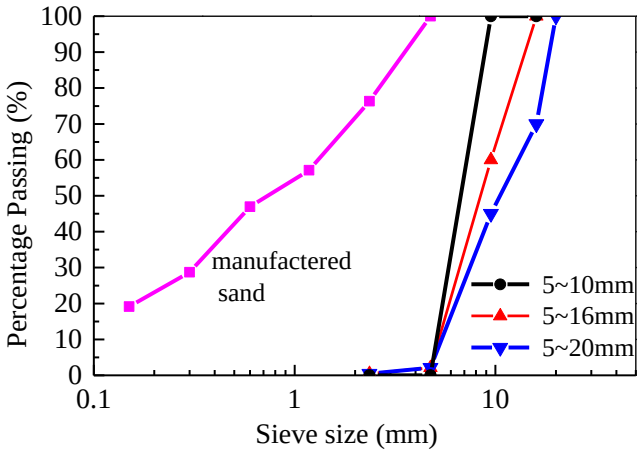


Figure 2. Particle size distributions of aggregate.

The fine aggregate was the manufactured sand crushed from limestone. The basic mechanical and physical properties were tested according Chinese standard JGJ 52 [37] and are presented in Table 3. The particle size distribution of manufactured sand is exhibited in Figure 2. Except for the over representation of particles with size less than 160 μm due to a high stone powder content of 7.3%, other distributions met the specification in Chinese standard JGJ 52 [37].

Table 3. Physical properties of manufactured sand.

Fineness Modulus	Apparent Density (kg/m^3)	Bulk Density (kg/m^3)		Void Content (%)		Stone Powder Content (%)
		Loose	Dense	Loose	Dense	
2.73	2740	1620	1850	40.9	32.5	7.3

2.2. Experimental Design

In this experiment, 252 groups of packing tests were designed. The volume fraction of steel fiber (v_f) ranged from 0 to 2.0% [38]. The sand ratio βs, expressed as in Equation (1), was the ratio of manufactured sand to the sum of aggregates and steel fiber by mass. Corresponding to each steel fiber volume fraction, the sand ratio ranged from 50% to 62%, with increments of 2%. Details of the experimental design are presented in Table 4.

$$\beta_s = \frac{m_s}{m_s + m_g + m_f}, \tag{1}$$

$$m_\mathrm{f} = 7850 v_\mathrm{f}, \tag{2}$$

where m_s, m_g, and m_f are the volumes of manufactured sand, coarse aggregate, and steel fiber in self-compacting SFRC.

Table 4. Experimental design.

Trials	Steel Fiber		Sand Ratio (%)	MPS of Coarse Aggregate (mm)
	Type	Volume Fraction v_f (%)		
00-10	-	0	50, 52, 54, 56, 58, 60, 62	10
00-16	-	0	50, 52, 54, 56, 58, 60, 62	16
00-20	-	0	50, 52, 54, 56, 58, 60, 62	20
HFa-10	HFa	0.4, 0.8, 1.2, 1.6, 2.0	50, 52, 54, 56, 58, 60, 62	10
HFa-16	HFa	0.4, 0.8, 1.2, 1.6, 2.0	50, 52, 54, 56, 58, 60, 62	16
HFb-16	HFb	0.4, 0.8, 1.2, 1.6, 2.0	50, 52, 54, 56, 58, 60, 62	16
HFc-16	HFc	0.4, 0.8, 1.2, 1.6, 2.0	50, 52, 54, 56, 58, 60, 62	16
HFc-20	HFc	0.4, 0.8, 1.2, 1.6, 2.0	50, 52, 54, 56, 58, 60, 62	20
CF-16	CF	0.4, 0.8, 1.2, 1.6, 2.0	50, 52, 54, 56, 58, 60, 62	16

2.3. Test Method

The premise of the experimental design was to keep the total volume of steel fiber and aggregates constant. The packing test was similar to the test method for the bulk density of coarse aggregates specified in Chinese code JGJ 52 [37] and ASTM C29 [39]. The raw materials of the coarse and fine aggregates and the steel fiber were weighed into a 20 L mixture and then uniformly mixed together. By using a bucket with a volume of 10 L (0.01 m^3), the mixture was filled in a free-falling manner to a height of 50 mm over the top of the bucket. After flattening the surface of the mixture by removing the protruding portion of the bucket surface, the sample in the bucket was weighed as m_m (kg). The bulk density ρ_bk (kg/m^3) and the void content of the steel fiber aggregate skeleton VC was calculated with Equations (3) and (4). Tests were repeated twice per group to reduce system error.

$$\rho_\mathrm{bk} = \frac{m_m}{0.01}, \tag{3}$$

$$VC = 1 - \frac{\rho_\mathrm{bk}}{\rho_\mathrm{a}}, \tag{4}$$

where ρ_a is the apparent density of the steel fiber aggregate mixture, which is the sum of the apparent densities of steel fiber, fine aggregate, and coarse aggregate by multiplying their own proportions in the mixture.

3. Effects of Fiber Factor on the Void Content of the Steel Fiber Aggregate Skeleton and the Optimal Sand Ratio

3.1. Relationship between Fiber Factor and Void Content of Steel Fiber Aggregate Skeleton

The bulk densities and void contents of the steel fiber aggregate skeleton are listed in Appendix A Table A1. Figure 3 shows the relationship of fiber factor λ_f and the void content VC of the steel fiber aggregate skeleton. Fiber factor λ_f is the product of the volume fraction v_f with aspect ratio l_f/d_f for the steel fiber, i.e., $\lambda_f = v_f \cdot l_f/d_f$. It can be seen that VC is linearly correlated with fiber factor λ_f for all test samples. The relationship between VC and λ_f can be expressed as in Equation (5).

$$VC = (1 + \alpha_{VC}\lambda_f)VC_0 \quad (5)$$

where VC_0 is the void content of the granular aggregate skeleton, which is related to the maximum particle size and grading of the coarse aggregate [1]; α_{VC} is a fitness parameter, which is listed in Table 5.

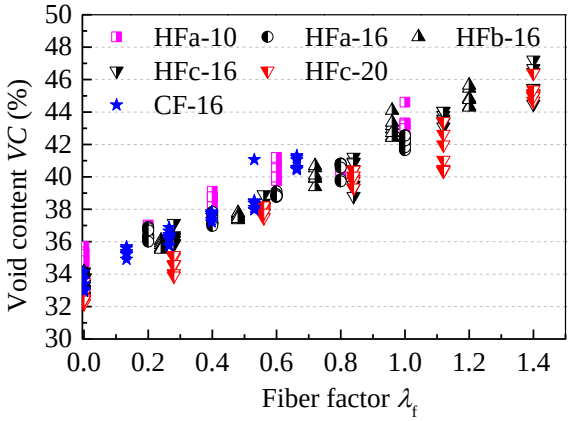


Figure 3. Changes of void content VC with a varying fiber factor λ_f.

Table 5. Statistical results of the parameter α_{VC}.

Item		HFa-10	HFa-16	HFb-16	HFc-16	HFc-20	CF-16
Fitness	Number	42	42	42	42	42	42
	Ratio of fiber length to MPS	2.500	1.563	1.875	2.188	1.750	2.425
	Parameter α_{VC}	0.227	0.275	0.291	0.267	0.265	0.329
	Standard Error	0.004	0.005	0.003	0.004	0.004	0.007
	Adjusted R-Square	0.953	0.946	0.987	0.974	0.968	0.943
Proposed	Parameter α_{VC}			0.27			0.33

When the MPS of the coarse aggregate was 10 mm, the fitness values of α_{VC} (Table 5) indicated that with the hooked-end steel fibers, VC showed a small increase with the increase of fiber factor λ_f, while large increases were seen for VC when the MPS of the coarse aggregate measured 16 and 20 mm. Due to the larger specific surface area of the coarse aggregate with MPS = 10 mm, a larger volume of binder paste was needed to achieve flowability for fresh self-compacting SFRC. Therefore, for the steel fiber aggregate skeletons with MPS = 16 and 20 mm for the coarse aggregate, the value of α_{VC} was larger than the mean value of α_{VC} = 0.27. Meanwhile, a large α_{VC} value was obtained for the steel fiber aggregate skeleton with the crimped steel fiber. There were many more voids between the crimped steel fibers and aggregates due to their decreased contact areas. For the proposed values of α_{VC}, Figure 4 presents the good agreement between the tested and calculated void contents of the steel fiber aggregate skeleton.

The binder paste volume in the concrete mixture could be divided into two parts, namely the void volume of the granular skeleton and the margin binder paste [1]. The former is used for filling the void of the granular skeleton, while the latter is used for lubricating the granular skeleton in fresh concrete to maintain suitable workability. Assuming the volume ratio of the margin binder paste to the total binder paste is constant, the rational volume content BP of binder paste for self-compacting SFRC compared with reference SCC can be expressed as Equation (6):

$$BP = (1 + \alpha_{VC}\lambda_f)BP_0, \tag{6}$$

where BP_0 is the volume content of binder paste for reference self-compacting concrete without steel fiber (SCC).

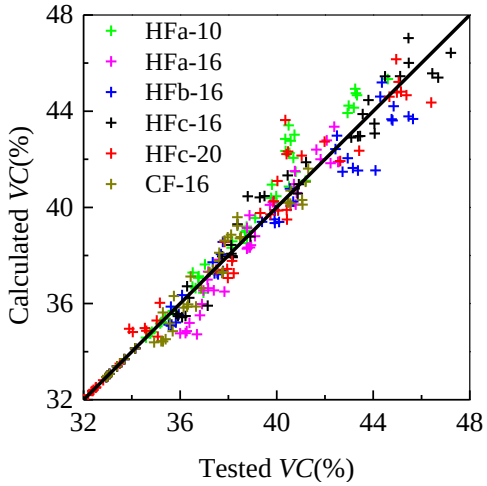


Figure 4. Comparison of tested and calculated values of void content *VC*.

Ignoring the volume changes for water and binder materials in the mixing process of self-compacting SFRC, the volume fraction of the binder paste is the sum of the volume fractions of the water and binder materials. Thus, Equation (6) is translated into Equation (7):

$$V_w + V_b = (1 + \alpha_{VC}\lambda_f)(V_{w0} + V_{b0}), \tag{7}$$

where V_w and V_b are the volume fractions of water and binder for self-compacting SFRC; V_{w0} and V_{b0} are the volume fractions of water and binder for reference SCC.

Ignoring the contribution of steel fiber to the compressive strength of self-compacting SFRC, the water-to-binder ratio by mass of self-compacting SFRC is the same as the referenced SCC and the same goes for the water-to-binder ratio by volume. That is,

$$\frac{V_w}{V_b} = \frac{V_{w0}}{V_{b0}}, \tag{8}$$

combined with Equations (7) and (8), the volume fractions of binder materials can be written as:

$$V_b = (1 + \alpha_{VC}\lambda_f)V_{b0}, \tag{9}$$

By dividing the density of the binder material in both sides of Equation (9), the binder content of self-compacting SFRC can be expressed as:

$$m_{bf} = (1 + \alpha_{VC}\lambda_f)m_{b0}, \tag{10}$$

where m_{bf} is the rational binder content of self-compacting SFRC and m_{b0} is the binder content of reference SCC.

3.2. The Optimal Sand Ratios

The variations of void content *VC* of the steel fiber aggregate skeleton with sand ratio β_f are shown in Figure 5. *VC* slightly decreased with increases of the sand ratio, while the fluctuation range increased with the fiber factor. Considering the beneficial effects of coarse aggregate dosage on the basic mechanical properties and volume stability of hardened concrete, the sand ratio should be as small as possible. Thus, the sand ratio corresponding to a significant decrease of the *VC* trend was determined as the optimal sand ratio. As an example, the deterministic process for optimal sand ratios for HFb-16 is presented in Figure 5, where the optimal sand ratios are drawn as black dots.

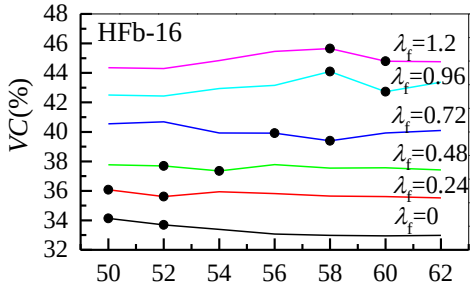


Figure 5. The deterministic process for optimal sand ratios for HFb-16.

Figure 6 presents the optimal sand ratio changes with fiber factor λ_f, for which the fitness formula is:

$$\beta_f^0 = \beta_0\left(1 + \alpha_\beta \lambda_f\right), \tag{11}$$

where β_f^0 is the rational sand ratio of self-compacting SFRC, β_0 is the sand ratio of reference SCC with the same raw materials and workability, and α_β is a fitness parameter. Here, α_β = 0.11, as per the fitness test results.

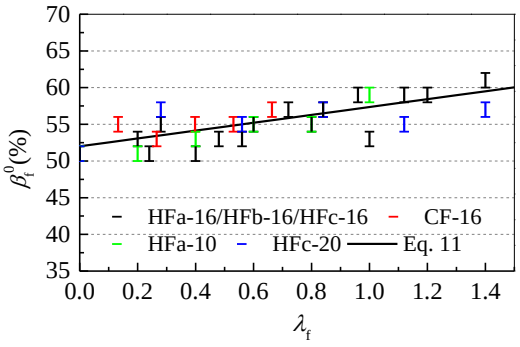


Figure 6. The relationship between the rational sand ratio β_f^0 and fiber factor λ_f.

4. Design Procedure for Mix Proportion of Self-Compacting SFRC

Based on the above research and previous studies [3,35,36,40], the mix design procedure for self-compacting SFRC is summarized as follows:

(1) Select the raw materials and determine the workability of fresh self-compacting SFRC;

(2) By fixing the designed cubic compressive strength $f_{cu,0}$ and the designed tensile strength $f_{ft,0}$, the volume fraction of steel fiber v_f can be calculated by Equations (12) [3,35,36] and (13) [40]:

$$f_{ft,0} = (1 + \alpha_{tb}\alpha_{te}\lambda_f) f_{t,0}, \tag{12}$$

$$f_{t,0} = \frac{(0.65 f_{cu,0} - 8)^{2/3}}{3}, \tag{13}$$

where $f_{t,0}$ is the tensile strength of reference SCC with the same water-to-binder ratio, α_{te} is the coefficient related to the effective fiber distribution, α_{tb} is a coefficient colligated the other factors influencing the bridging effect of steel fibers on tensile strength of self-compacting SFRC.

(3) The water-to-binder ratio *w/b* of self-compacting SFRC can be calculated by Equation (14) [41]:

$$w/b = \frac{\alpha_a f_b}{f_{cu,0} + \alpha_a \alpha_b f_b}, \tag{14}$$

where α_a and α_b are coefficients mainly related to the type of coarse aggregate and concrete; $\alpha_a = 0.270$ and $\alpha_b = -0.522$; f_b is the compressive strength of the binder material at curing age of 28 days.

(4) By using the absolute volume method, the detailed mix proportion of reference SCC with the same *w/b* as the self-compacting SFRC can be determined. Packing tests for aggregates with different sand ratios are conducted to obtain the optimal sand ratio β_0 and volume fraction for the coarse aggregate and fine aggregate;

(5) The binder content of self-compacting SFRC m_{bf} is fixed using Equation (10). Thus, the dosages of cement and mineral admixtures can be calculated;

(6) Calculate the water content m_{wf} using Equation (15):

$$m_{wf} = \frac{m_{bf}}{w/b}, \tag{15}$$

(7) Calculate the rational sand ratio β_f^0 of self-compacting SFRC using Equation (11);

(8) Calculate the dosages of fine aggregate and coarse aggregate m_{sf} and m_{gf} using the absolute volume method, as follows:

$$\frac{m_{bf}}{\rho_b} + \frac{m_{wf}}{\rho_w} + \frac{m_{sf}}{\rho_s} + \frac{m_{gf}}{\rho_g} + v_f + 0.01\alpha = 1, \tag{16}$$

where ρ_b, ρ_w, ρ_s, and ρ_g are the densities of binder materials, water, fine aggregate, and coarse aggregate, respectively, expressed as kg/m^3; α is the air content of fresh self-compacting SFRC, expressed as a %.

(9) Determine the superplasticizer dosage based on the assessment of the required performance. Trial mixes with different dosages of superplasticizer should be carried out.

The workability and mechanical properties of self-compacting SFRC should satisfy the construction requirements. Otherwise, proper adjustments should be made until satisfactory results are achieved.

5. Verification for the Design of the Mix Proportions of Self-Compacting SFRC

5.1. Experimental Design

Eight groups of mixes were experimentally studied to verify the rationality of the mix proportion design method of self-compacting SFRC. The main parameters were the water-to-binder ratio *w/b* = 0.31, and the volume fractions of steel fiber v_f = 0%, 0.4%, 0.8%, 1.2%, 1.4% and 1.6%. As the same as the packing test of steel fiber-aggregate skeleton, the hooked-end steel fibers named as HFa, HFb and HFc, the crushed limestone with a maximum particle size of 16mm, and the manufactured sand were used. Grade P.O. 42.5 ordinary silicate cement and fly ash were used as the binder materials. Their physical and mechanical properties are tested according Chinese standard GB 175 [42] and GB/T51003 [43] and listed in Table 6, respectively. Tap water and PCA-I polycarboxylic high performance water-reducer with solid content as 24.1% and water-reducing rate greater than 28% were also used in this experiment. The designed strengths and detailed mix proportion of self-compacting SFRC are listed in Table 7.

Table 6. Physical and mechanical properties of cement and fly ash.

Cement								
Density (kg/m^3)	Fluidity of cement mortar (mm)	Water requirement of normal consistency (%)	Setting time (min)		Flexural strength (MPa)		Compressive strength f_{ce} (MPa)	
			Initial	Final	3d	28d	3d	28d
3085	137	26.4	160	245	6.17	9.43	29.4	54.7
Fly Ash								
Density (kg/m^3)	Fineness (45μm, %)	Water demand ratio (%)	Strength activity index (%)		Loss on ignition (%)		Class	
2349	10	98	80.9		1.9		II	

Table 7. Detailed mix proportion of self-compacting steel-fiber-reinforced concrete (SFRC).

Mixtures		**Reference SCC**	**HFb04**	**HFb08**	**HFb12**	**HFb14**	**HFb16**	**HFa12**	**HFc12**
Designed compressive strength $f_{cu,0}$ (MPa)		50	50	50	50	50	50	50	50
Designed tensile strength $f_{ft,0}$ (MPa)		2.93	3.28	3.63	3.98	4.16	4.34	3.81	4.16
w/*b*		0.31	0.31	0.31	0.31	0.31	0.31	0.31	0.31
Sand ratio β_s (%,by mass)		50	52	54	56	57	58	55	57
Fly ash content (%,by mass)		30	30	30	30	30	30	30	30
Steel fiber	Type	-	HFb	HFb	HFb	HFb	HFb	HFa	HFc
	v_f (%)	0	0.4	0.8	1.2	1.4	1.6	1.2	1.2
	λ_f	0	0.24	0.48	0.72	0.84	0.96	0.6	0.84
Water (kg/m^3)		192	201	210	219	223	228	214	223
Cement (kg/m^3)		433	454	474	494	504	514	484	504
Fly ash (kg/m^3)		186	194	203	214	216	220	207	216
Coarse aggregate (kg/m^3)		751	675	601	527	491	455	553	502
Manufactured sand(kg/m^3)		751	763	774	783	788	792	784	782
Water reducer (kg/m^3)		5.57	5.51	5.42	5.30	5.40	5.51	5.19	5.40
Steel fiber (kg/m^3)		0	31.4	62.8	94.2	109.9	125.6	94.2	94.2

5.2. Performances of Fresh Self-Compacting SFRC

The air content of fresh self-compacting SFRC was tested using the pressure method without vibratory compaction, referring to Chinese code GB/T 50080 [44] and ASTM C231 [45]. As presented in Figure 7, the air content increased with the volume fraction of the steel fiber. The air content of HF-16 was about 76% higher than that of reference SCC. The addition of more steel fibers would introduce more air into the fresh self-compacting SFRC. This is consistent with the studies of Ding and Yang [46] and Miao et al [47].

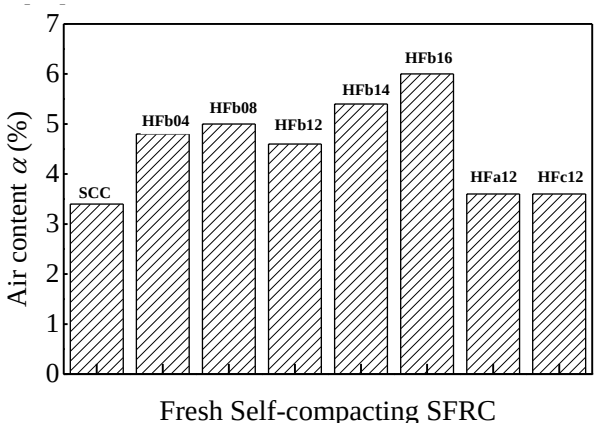


Figure 7. Air content of fresh self-compacting SFRC.

The workability of fresh self-compacting SFRC was evaluated by slump flow and flow time T_{500} tests, in accordance with Chinese standard JGJ/T 283 [29], which is identical to ASTM C1611 [48] and ASTM C 1621 [49]. The test results are presented in Table 8 and the pictures for the slump flow test are shown in Figure 8. The slump flow and flow time T_{500} ranged within 560–685 mm and 4.33–6.71 s, respectively. For self-compacting SFRC with HFb, the slump flow values were relatively stable at v_f = 0.4–1.4%, decreasing to v_f = 1.6%. In the same condition at v_f = 1.2%, the slump flow decreased slightly with the increased fiber length. In general, the slump flow of self-compacting SFRC fits the filling ability level SF1 (slump flow = 550–655mm) or level SF2 (slump flow = 660–755mm), while T_{500} fits the the filling ability level VS1 (2 s ≤ T_{500} ≤ 8 s). This means that the fresh self-compacting SFRC is suitable for concrete structures and conventional reinforced concrete structures [29].

Table 8. Test results for fresh self-compacting SFRC.

Test Type	Experiment No.							
	SCC	HFb04	HFb08	HFb12	HFb14	HFb16	HFa12	HFc12
Slump-flow (mm)	655	685	635	660	665	595	630	560
T_{500} (s)	5.38	5.36	4.44	5.4	6.28	6.37	4.33	6.71

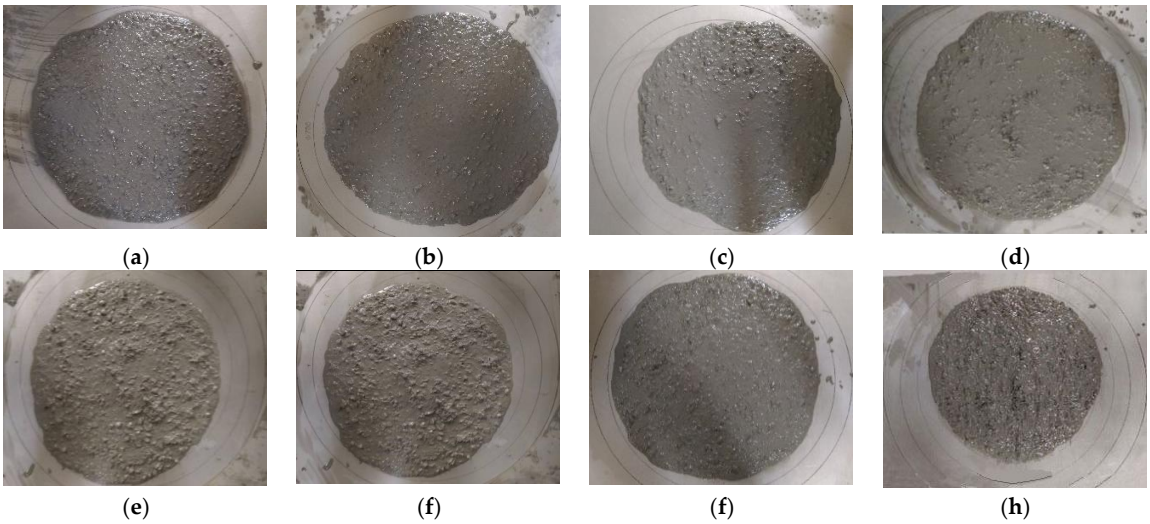


Figure 8. Pictures of slump flow tests. (**a**) concrete cake of reference SCC, (**b**) concrete cake of HFb04, (**c**) concrete cake of HFb08, (**d**) concrete cake of HFb12, (**e**) concrete cake of HFb14, (**f**) concrete cake of HFb16, (**g**) concrete cake of HFa12, (**h**) concrete cake of HFc12.

5.3. Density of Self-Compacting SFRC

Density is a macro index evaluating the compactness of hardened concrete. Figure 9 displays the variations of the density of hardened self-compacting SFRC, along with fiber factor λ_f. The density ratios of self-compacting SFRC to reference SCC were in the range of 97.0–100.1%. The addition of steel fiber showed little influence on the compactness of hardened self-compacting SFRC in this experiment, meaning that satisfactory compactness was obtained using the proposed mix design method for self-compacting SFRC.

5.4. Mechanical Properties of Self-Compacting SFRC

The cubic compressive strength f_{cu} and splitting tensile strength f_{ft} of self-compacting SFRC were tested at 28 days using cubic specimens with dimensions of 150 mm, according to the specifications of Chinese Standard GB/T50081 [50], which is identical to British Standards BS EN 12390-3 [51] and BS EN12390-6 [52]. The test results are presented in Table 9.

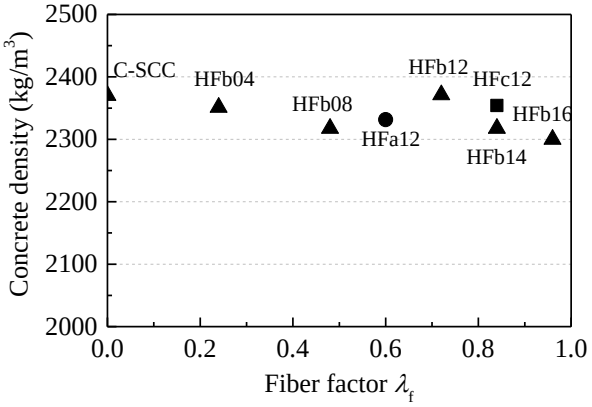


Figure 9. Variations of the density, along with the fiber factor.

Table 9. The tested strengths and ratios with the designed value.

No.	Reference SCC	HFb04	HFb08	HFb12	HFb14	HFb16	HFa12	HFc12
Compressive strength f_{cu} (MPa)	54.5	52.3	55.8	60.4	56.5	62.2	61.8	60.9
Splitting tensile strength f_{ft} (MPa)	3.19	4.28	4.39	4.60	4.17	–	4.35	4.35
$f_{cu}/f_{cu,0}$	1.090	1.046	1.116	1.208	1.130	1.244	1.236	1.218
$f_{ft}/f_{ft,0}$	1.089	1.304	1.208	1.154	1.002	-	1.142	1.046

The tested cubic compressive strength f_{cu} and splitting tensile strength f_{ft} of self-compacting SFRC were in the ranges of 52.3–62.2 MPa and 3.19–4.60 MPa, respectively, all of which increased with the fiber factor. The values for tested to designed cubic compressive strength ratio $f_{cu}/f_{cu,0}$ ranged from 1.046 to 1.244, and those of tested to designed splitting tensile strength ratio $f_{ft}/f_{ft,0}$ ranged from 1.002 to 1.304. The discreteness values for compressive strength and tensile strength were both acceptable for the mix proportion design of self-compacting SFRC.

Considering the performances of fresh and hardened self-compacting SFRC, the design method is suitable for the mix proportion design of self-compacting SFRC.

6. Conclusions

This paper presents a mix design method for self-compacting SFRC based on packing tests for the steel fiber and aggregate mixture. Based on the packing test results, the fiber factor shows a positive correlation with the void content of the steel fiber aggregate skeleton. Taking the reference void content of the aggregate skeleton and fiber factor into account, a calculation model is proposed for the void content of the steel fiber aggregate skeleton. Meanwhile, a formula for the binder content of self-compacting SFRC is established, considering the fiber factor and the binder content of the reference SCC.

The rational sand ratio of self-compacting SFRC is positively related to the fiber factor. Taking the sand ratio of the reference SCC and fiber factor into account, a forecast model is proposed for the rational sand ratio of the self-compacting SFRC.

The procedure for the mix proportion design of self-compacting SFRC is outlined. The volume fraction of the steel fiber is chosen according to the designed tensile strength in th self-compacting SFRC. Combined with binder content formulas and the rational sand ratio proposed in this paper, the absolute volume method for the mix proportion is used to determine the aggregate contents of the self-compacting SFRC.

The adaptability and practicability of the mix design method for self-compacting SFRC are confirmed by the verification tests of eight groups of self-compacting SFRC mixtures. The slump flow and flow time T_{500} performance results for fresh self-compacting SFRC with the volume fraction of steel fiber in the range of 0–1.6% are acceptable. The air content of fresh self-compacting SFRC

increases with the fiber factor. The tested compressive and splitting tensile strengths increase with the fiber factor, agreeing well with the designed values.

Author Contributions: Methodology, X.D. and M.Z., and J.L.; investigation and data curation, X.D., P.S., and C.L; writing—original draft preparation, X.D. and M.Z.; writing—review and funding acquisition, X.D., J.L., and C.L. All authors have read and agreed to the published version of the manuscript.

Funding: This research was funded by the Key Scientific and Technological Research Project of University in Henan, China (grant numbers 20A560015 and 17A560025), Attracting Foreign Talents Fund of Henan, China (grant number YWZ2018-6-HS2), State Key Research and Development Plan, China (grant number 2017YFC0703904), and Innovative Sci-Tech Team of Eco-building Material and Structural Engineering of Henan Province, China (grant number YKRZ-6-066).

Conflicts of Interest: The authors declare no conflict of interest.

Appendix A

Table A1. The packing test results for steel fiber aggregate mixtures.

No.	v_f (%)	Test Results	Sand Ratios (%)						
			50	52	54	56	58	60	62
00-10	0	ρ_b (kg/m^3)	1760.3	1769.0	1774.8	1773.0	1786.0	1790.8	1784.3
		VC (%)	35.7	35.4	35.2	35.2	34.8	34.6	34.8
00-16	0	ρ_b (kg/m^3)	1803.0	1815.3	1823.5	1832.3	1834.5	1835.8	1834.8
		VC (%)	34.1	33.7	33.4	33.1	33.0	32.9	33.0
00-20	0	ρ_b (kg/m^3)	1847.3	1856.3	1839.3	1820.5	1851.5	1848.0	1850.3
		VC (%)	32.5	32.2	32.8	33.5	32.4	32.5	32.4
HFa-10	0.4	ρ_b (kg/m^3)	1744.3	1758.3	1752.0	1751.5	1755.0	1746.0	1758.5
		VC (%)	37.0	36.5	36.7	36.8	36.6	37.0	36.5
	0.8	ρ_b (kg/m^3)	1707.8	1717.5	1719.5	1717.8	1717.0	1734.5	1734.0
		VC (%)	39.1	38.8	38.7	38.7	38.8	38.1	38.2
	1.2	ρ_b (kg/m^3)	1682.3	1671.0	1690.0	1709.3	1710.3	1704.0	1704.5
		VC (%)	40.8	41.2	40.5	39.8	39.8	40.0	40.0
	1.6	ρ_b (kg/m^3)	1710.8	1704.3	1708.5	1714.5	1710.0	1705.5	1714.3
		VC (%)	40.5	40.7	40.6	40.4	40.5	40.7	40.4
	2.0	ρ_b (kg/m^3)	1618.8	1655.8	1653.8	1655.0	1657.3	1664.5	1663.3
		VC (%)	44.6	43.3	43.3	43.3	43.2	42.9	43.0
HFa-16	0.4	ρ_b (kg/m^3)	1747.8	1750.0	1762.0	1765.0	1766.5	1753.5	1772.5
		VC (%)	36.9	36.8	36.4	36.3	36.2	36.7	36.0
	0.8	ρ_b (kg/m^3)	1749.0	1761.0	1762.0	1761.3	1754.8	1742.8	1766.5
		VC (%)	37.6	37.2	37.1	37.2	37.4	37.8	37.0
	1.2	ρ_b (kg/m^3)	1734.8	1737.5	1728.5	1733.3	1734.3	1737.8	1736.8
		VC (%)	38.9	38.8	39.1	38.9	38.9	38.8	38.8
	1.6	ρ_b (kg/m^3)	1703.8	1704.8	1701.8	1728.8	1702.8	1708.8	1732.0
		VC (%)	40.8	40.7	40.8	39.8	40.8	40.6	39.7
	2.0	ρ_b (kg/m^3)	1679.5	1688.0	1699.8	1695.0	1674.5	1683.8	1675.3
		VC (%)	42.4	42.1	41.6	41.8	42.6	42.2	42.5

Table A1. *Cont.*

No.	v_f (%)	Test Results	Sand Ratios (%)						
			50	**52**	**54**	**56**	**58**	**60**	**62**
HFb-16	0.4	ρ_b (kg/m^3)	1770.3	1783.0	1774.0	1777.5	1782.3	1783.0	1785.5
		VC (%)	36.1	35.6	35.9	35.8	35.6	35.6	35.5
	0.8	ρ_b (kg/m^3)	1744.5	1746.5	1756.0	1744.3	1750.8	1750.0	1754.0
		VC (%)	37.8	37.7	37.3	37.8	37.5	37.6	37.4
	1.2	ρ_b (kg/m^3)	1688.8	1685.1	1705.8	1706.3	1720.5	1706.0	1701.3
		VC (%)	40.6	40.7	39.9	39.9	39.4	39.9	40.1
	1.6	ρ_b (kg/m^3)	1656.0	1657.8	1643.8	1638.0	1612.3	1649.8	1632.3
		VC (%)	42.5	42.4	42.9	43.2	44.1	42.7	43.4
	2.0	ρ_b (kg/m^3)	1625.5	1627.3	1612.3	1595.3	1590.3	1613.5	1614.5
		VC (%)	44.4	44.3	44.8	45.5	45.6	44.8	44.8
HFc-16	0.4	ρ_b (kg/m^3)	1764.5	1762.3	1741.3	1777.0	1766.5	1770.3	1775.0
		VC (%)	36.3	36.4	37.1	35.8	36.2	36.1	35.9
	0.8	ρ_b (kg/m^3)	1727.8	1713.3	1735.0	1734.8	1733.8	1733.5	1745.3
		VC (%)	38.4	38.9	38.1	38.1	38.2	38.2	37.7
	1.2	ρ_b(kg/m^3)	1670.5	1691.5	1678.8	1680.0	1717.8	1723.0	1736.8
		VC (%)	41.2	40.5	40.9	40.9	39.5	39.3	38.8
	1.6	ρ_b (kg/m^3)	1620.3	1626.8	1613.5	1613.3	1629.8	1639.8	1632.3
		VC (%)	43.8	43.6	44.0	44.1	43.5	43.1	43.4
	2.0	ρ_b (kg/m^3)	1595.3	1547.3	1595.0	1568.3	1604.8	1561.8	1622.0
		VC (%)	45.5	47.2	45.5	46.4	45.1	46.7	44.5
HFc-20	0.4	ρ_b (kg/m^3)	1812.5	1797.8	1799.0	1795.5	1826.3	1830.3	1810.8
		VC (%)	34.5	35.1	35.0	35.2	34.0	33.9	34.6
	0.8	ρ_b (kg/m^3)	1739.5	1738.8	1734.0	1742.5	1732.3	1752.0	1744.5
		VC (%)	38.0	38.0	38.2	37.8	38.2	37.5	37.8
	1.2	ρ_b (kg/m^3)	1692.5	1692.3	1707.3	1703.0	1711.0	1702.3	1722.5
		VC (%)	40.4	40.4	39.9	40.0	39.7	40.1	39.3
	1.6	ρ_b(kg/m^3)	1630.8	1652.3	1670.0	1714.5	1696.0	1711.5	1713.3
		VC (%)	43.4	42.6	42.0	40.4	41.0	40.5	40.4
	2.0	ρ_b (kg/m^3)	1603.8	1569.5	1606.5	1609.3	1617.0	1608.5	1597.8
		VC (%)	45.2	46.4	45.1	45.0	44.7	45.0	45.4
CF-16	0.4	ρ_b (kg/m^3)	1792.0	1784.0	1781.0	1789.0	1794.0	1802.0	1792.0
		VC (%)	35.3	35.6	35.7	35.4	35.2	34.9	35.3
	0.8	ρ_b (kg/m^3)	1781.0	1769.0	1800.0	1784.0	1775.0	1789.0	1785.0
		VC (%)	36.4	36.9	35.7	36.3	36.7	36.1	36.3
	1.2	ρ_b (kg/m^3)	1763.0	1769.0	1769.0	1776.0	1765.0	1766.0	1780.0
		VC (%)	37.8	37.6	37.6	37.4	37.8	37.7	37.2
	1.6	ρ_b (kg/m^3)	1695.0	1769.0	1769.0	1776.0	1765.0	1766.0	1780.0
		VC (%)	41.1	38.4	38.4	38.1	38.5	38.5	38.0
	2.0	ρ_b (kg/m^3)	1709.0	1712.0	1729.0	1716.0	1732.5	1729.3	1731.8
		VC (%)	41.3	41.2	40.6	41.1	40.5	40.6	40.5

References

1. Larrard, F.D. *Concrete Mixture Proportioning: A Scientific Approach*; Routledge: New York, NY, USA, 1999.
2. Ghanem, H.; Ayman, Y.O.; Dandachy, T.M. The impact of steel fibers on the properties of self compacting concrete. International Congress and Exhibition "Sustainable Civil Infrastructures": Innovative Infrastructure Geotechnology. In Proceedings of the GeoMEast 2018: Advances and Challenges in Structural Engineering, Cairo, Egypt, 24–28 November 2018; pp. 138–150.
3. Ding, X.X.; Li, C.Y.; Han, B.; Lu, Y.Z.; Zhao, S.B. Effects of different deformed steel-fibers on preparation and fundamental properties of self-compacting SFRC. *Constr. Build. Mater.* **2018**, *168*, 471–481. [CrossRef]
4. Ding, X.X.; Li, C.Y.; Li, Y.Z.; Lu, Y.Z.; Song, C.; Zhao, S.B. Experimental and numerical study on stress-strain behavior of self-compacting SFRC under uniaxial compression. *Constr. Build. Mater.* **2018**, *185*, 30–38. [CrossRef]
5. Huang, K.J.; Li, G.F.; Wang, Y.G.; Wei, Y. Properties of high strength self-compacting steel fiber reinforced concrete used in bridge steel-mixes union section. *J. Wuhan Univ. Technol.* **2013**, *35*, 107–111, 116.
6. Mastali, M.; Dalvand, A. Fresh and hardened properties of self-compacting concrete reinforced with hybrid recycled steel–polypropylene fiber. *J. Mater. Civil.* **2017**, *29*, 04017012. [CrossRef]
7. Mastali, M.; Dalvand, A. Use of silica fume and recycled steel fibers in self-compacting concrete (SCC). *Constr. Build. Mater.* **2016**, *30*, 196–209. [CrossRef]
8. Wang, C.; Li, H.B.; Yang, C.H.; Ye, J.X.; Bai, G. Preparation technology of fiber toughened self-compacting high-strength concrete. *J. Civil. Archit. Environ. Eng.* **2013**, *35*, 129–134.
9. Basheerudeen, A.; Anandan, S. Simplified mix design procedures for steel fibre reinforced self-compacting concrete. *Eng. J.* **2015**, *19*, 22–24. [CrossRef]
10. Sahmaran, M.; Yaman, I.O. Hybrid fiber reinforced self-compacting concrete with a high-volume coarse fly ash. *Constr. Build. Mater.* **2007**, *21*, 150–156. [CrossRef]
11. Athiyamaan, V.; Mohan Ganesh, G. Experimental, statistical and simulation analysis on impact of micro steel—Fibres in reinforced SCC containing admixtures. *Constr. Build. Mater.* **2020**, *246*, 118450. [CrossRef]
12. Alberti, M.G.; Enfedaque, A.; Gálvez, J.C.; Cortez, A. Optimisation of fibre reinforcement with a combination strategy and through the use of self-compacting concrete. *Constr. Build. Mater.* **2020**, *235*, 117289. [CrossRef]
13. Tsai, C.T.; Li, L.S.; Chang, C.C.; Hwang, C.L. Durability design and application of steel fiber reinforced concrete in Taiwan. *Arab. J. Sci. Eng.* **2009**, *34*, 57–79.
14. Grunewald, S. Performance Based Design of Self-Compacting Steel Fiber Reinforced Concrete. Ph.D. Thesis, Delft University of Technology, Delft, The Netherlands, 2004.
15. Yu, A.B.; Standish, N.; McLean, A. Porosity calculation of binary mixtures of non-spherical particles. *J. Am. Ceram. Soc.* **1993**, *76*, 2813–2816. [CrossRef]
16. Ferrara, L.; Park, Y.D.; Shah, S.P. A method for mix-design of fiber-reinforced self-compacting concrete. *Cement. Concrete. Res.* **2007**, *37*, 957–971. [CrossRef]
17. Saak, A.W.; Jennings, H.M.; Sha, S.P. New methodology for designing self-compacting concrete. *ACI Mater. J.* **2001**, *98*, 429–439.
18. Gueciouer, D.; Youcef, G.; Tarek, N. Rheological and mechanical optimization of a steel fiber reinforced self-compacting concrete using the design of experiments method. *Eur. J. Environ. Civ. En.* **2019**, *11*, 1–22. [CrossRef]
19. Fernandes, P.A.L.; Veludo., J.; Almeida, N.; Baptista, J.; Rodrigues, H. Study of a self-compacting fiber-reinforced concrete to be applied in the precast industry. *Innov. Infrast. Sol.* **2018**, *28*, 1–11. [CrossRef]
20. Pereira, E.N.B.; Barros, J.A.O.; Camões, A. Steel fiber-reinforced self-compacting concrete: Experimental research and numerical simulation. *J. Struct. Eng.* **2008**, *134*, 1310–1321. [CrossRef]
21. Barros, J.; Pereira, E.; Santos, S. Lightweight panels of steel fiber-reinforced self-compacting concrete. *J. Mater. Civ. Eng.* **2007**, *19*, 295–304. [CrossRef]
22. He, X.B.; Liu, S.X.; Liu, Y.; Jia, Q.B. A new two-step mix proportion design of micro-steel fiber reinforced self-compacting concrete. *J. Build. Mater.* **2020**, *1*, 56–63.
23. de Oliveira, L.A.P.; Gomes, J.P.C.; Bernardo, L.F.A.; Ramos, M.M.M. Evaluation of dry mortar ratio as mix design parameter for steel fibre reinforced self compacting concrete. *Constr. Build. Mater.* **2013**, *40*, 642–649. [CrossRef]

24. Mahapatra, C.K.; Barai, S.V. Hybrid fiber reinforced self compacting concrete with fly ash and colloidal nano silica: A systematic study. *Constr. Build. Mater.* **2018**, *160*, 828–838. [CrossRef]
25. Ghorbani, S.; Sharifi, S.; Rokhsarpour, H.; Shoja, S.; Gholizadeh, M.; Rahmatabad, M.A.D.; Brito, J.D. Effect of magnetized mixing water on the fresh and hardened state properties of steel fibre reinforced self-compacting concrete. *Constr. Build. Mater.* **2020**, *248*, 118660. [CrossRef]
26. BIBM; CEMBUREAU; EFCA; EFNARC; ERMCO. *The European Guidelines for Self-Compacting Concrete Specification, Production and Use*; EFNARC, Association House: Surrey, UK, 2005; p. 18.
27. European Committee for Standardization. *Fibres for Concrete. Steel Fibres: Definitions, Specifications & Conformity, BS EN 14889-1-2006*; British Standards Institution: London, UK, 2006.
28. European Committee for Standardization. *Concrete Part 9 Additional Rules for Self-Compacting Concrete (SCC), BS EN 206-9-2010*; British Standards Institution: London, UK, 2010.
29. Ministry of Housing and Urban-Rural Development of the People's Republic of China. *Technical Specification for Application of Self-Compacting Concrete, JGJ/T 283-2012*; China Architecture & Building Press: Beijing, China, 2012.
30. China Association of Engineering Construction Standardization. *Test Methods for Steel Fiber Reinforced Concrete, CECS 13:2009*; China Planning Press: Beijing, China, 2010.
31. Ministry of Housing and Urban-Rural Development of the People's Republic of China. *Steel Fiber Reinforced Concrete, JG/T 472-2015*; China Architecture & Building Press: Beijing, China, 2015.
32. Ministry of Housing and Urban-Rural Development of the People's Republic of China. *Technical Specification for Application of Fiber Reinforced Concrete, JGJ/T 221-2010*; China Building Industry Press: Beijing, China, 2010.
33. Ding, X.X.; Li, C.Y.; Xu, Y.Y.; Li, F.L.; Zhao, S.B. Experimental study on long-term compressive strength of concrete with manufactured sand. *Constr. Build. Mater.* **2016**, *108*, 67–73. [CrossRef]
34. Zhao, S.B.; Ding, X.X.; Zhao, M.S.; Li, C.Y.; Pei, S.W. Experimental study on tensile strength development of concrete with manufactured sand. *Constr. Build. Mater.* **2017**, *138*, 247–253. [CrossRef]
35. Zhao, M.L.; Ding, X.X.; Li, J.; Law, D. Numerical analysis of mix proportion of self-compacting concrete compared to ordinary concrete. *Key Eng. Mater.* **2018**, *789*, 69–75. [CrossRef]
36. Ding, X.X.; Zhao, M.L.; Zhou, S.Y.; Fu, Y.; Li, C.Y. Statistical analysis and preliminary study on the mix proportion design of self-compacting SFRC. *Materials* **2019**, *12*, 637. [CrossRef] [PubMed]
37. Ministry of Housing and Urban-Rural Development of the People's Republic of China. *Standard for Technical Requirements and Test Method of Sand and Crushed Stone (or Gravel) for Ordinary Concrete, JGJ 52-2006*; China Planning Press: Beijing, China, 2006.
38. Zhao, M.L.; Li, J.; Law, D. Effects of flowability on SFRC fibre distribution and properties. *Magaz. Concr. Res.* **2017**, *69*, 1043–1054. [CrossRef]
39. American Society of Testing Materials. *Standard Test Method for Bulk Density ("Unit Weight") and Voids in Aggregate, ASTM C29/C29M—17a*; ASTM International: West Conshohocken, PA, USA, 2017.
40. Vilanova, A.; Fernandez-Gomez, J.; Landsberger, G.A. Evaluation of the mechanical properties of self compacting concrete using current estimating models: Estimating the modulus of elasticity, tensile strength and modulus of rupture of self compacting concrete. *Constr. Build. Mater.* **2011**, *25*, 3417–3426. [CrossRef]
41. Ministry of Housing and Urban-Rural Development of the People's Republic of China. *Specification for Mix Proportion Design of Ordinary Concrete, JGJ 55-2011*; China Building Industry Press: Beijing, China, 2011.
42. Standardization Administration of the People's Republic of China. *Common Portland Cement, GB175-2007*; China Building Industry Press: Beijing, China, 2007.
43. Ministry of Housing and Urban-Rural Development of the People's Republic of China. *Technical Code for Application of Mineral Admixture, GB/T51003-2014*; China Building Industry Press: Beijing, China, 2014.
44. Ministry of Housing and Urban-Rural Development of the People's Republic of China. *Standard for Test Method of Performance on Ordinary Fresh Concrete, GB/T 50080-2016*; China Building Industry Press: Beijing, China, 2016.
45. American Society of Testing Materials. *Standard Test Method for Air Content of Freshly Mixed Concrete by the Pressure Method, ASTM C231 C231M-2017a*; ASTM International: West Conshohocken, PA, USA, 2017.
46. Ding, Y.N.; Yang, N. Experimental study on fiber reinforced high performance concrete. *J. Shengyang Jianzhu Univ.* **2006**, *22*, 125–128.
47. Miao, B.Q.; Chern, J.C.; Yang, C.A. Influences of fiber content on properties of self-compacting steel fiber reinforced concrete. *J. Chin. Inst. Eng.* **2003**, *26*, 523–530. [CrossRef]

48. American Society of Testing Materials. *Standard Test Method for Slump Flow of Self-Consolidating Concrete, ASTM C1611-C1611M-2014*; ASTM International: West Conshohocken, PA, USA, 2014.
49. American Society of Testing Materials. *Standard Test Method for Passing Ability of Self-Consolidating Concrete by J-Ring, ASTM C1621_C1621M-2014*; ASTM International: West Conshohocken, PA, USA, 2014.
50. Ministry of Housing and Urban-Rural Development of the People's Republic of China. *Standard for Test Methods for Concrete Physical and Mechanical Properties, GB/T 50081-2019*; China Building Industry Press: Beijing, China, 2019.
51. European Committee for Standardization. *Testing hardened Concrete-Part 3: Compressive Strength of Test Specimens, BS EN 12390-3-2009*; European Committee for Standardization: London, UK, 2009.
52. European Committee for Standardization. *Testing Hardened Concrete-Part 6: Tensile Splitting Strength of Test Specimen, BS EN 12390-6-2009*; European Committee for Standardization: London, UK, 2009.



© 2020 by the authors. Licensee MDPI, Basel, Switzerland. This article is an open access article distributed under the terms and conditions of the Creative Commons Attribution (CC BY) license (http://creativecommons.org/licenses/by/4.0/).